A Protein Interaction Network for the Large Conductance Ca^{2+}-activated K^+ Channel in the Mouse Cochlea*

Thandavarayan Kathiresan‡, Margaret Harvey‡, Sandra Orchard§, Yoshihisa Sakai‡, and Bernd Sokolowski‡¶

The large conductance Ca^{2+}-activated K^+ or BK channel has a role in sensory/neuronal excitation, intracellular signaling, and metabolism. In the non-mammalian cochlea, the onset of BK during development correlates with increased hearing sensitivity and underlies frequency tuning in non-mammals, whereas its role is less clear in mammalian hearing. To gain insights into BK function in mammals, coimmunoprecipitation and two-dimensional PAGE, combined with mass spectrometry, were used to reveal 174 putative BKAPs from cytoplasmic and membrane/cytoskeletal fractions of mouse cochlea. Eleven BKAPs were verified using reciprocal coimmunoprecipitation, including annexin, apolipoprotein, calmodulin, hippocalcin, and myelin P0, among others. These proteins were immunocolocalized with BK in sensory and neuronal cells. A bioinformatics approach was used to mine databases to reveal binary partners and the resultant protein network, as well as to determine previous ion channel affiliations, subcellular localization, and cellular processes. The search for binary partners using the IntAct molecular interaction database produced a putative global network of 160 nodes connected with 188 edges that contained 12 major hubs. Additional mining of databases revealed that more than 50% of primary BKAPs had prior affiliations with K^+ and Ca^{2+} channels. Although a majority of BKAPs are found in either the cytoplasm or membrane and contribute to cellular processes that primarily involve metabolism (30.5%) and trafficking/scaffolding (23.6%), at least 20% are mitochondrial-related. Among the BKAPs are chaperonins such as calreticulin, GRP78, and HSP60 that, when reduced with siRNAs, alter BKα expression in CHO cells. Studies of BKα in mitochondria revealed compartmentalization in sensory cells, whereas heterologous expression of a BK-DEC splice variant cloned from cochlea revealed a BK mitochondrial candidate. The studies described herein provide insights into BK-related functions that include not only cell excitation, but also cell signaling and apoptosis, and involve proteins concerned with Ca^{2+} regulation, structure, and hearing loss. *Molecular & Cellular Proteomics 8:1972–1987, 2009.*

BK[1] channels act as sensors for membrane voltage and intracellular Ca^{2+}, thereby linking cell excitability, metabolism, and signaling. BK channels, also known as Slo, are large conductance channels (100–300 pS) (1) composed of four α-subunits that are regulated by four auxiliary β-subunits. The α-subunit of the BK channel has six to seven transmembrane-spanning regions (S0–S6) where the S0 domain places the N terminus extracellularly as a binding site for the beta subunit. The transmembrane domains S1-S4 are responsible for sensing voltage changes, whereas the pore forming region, between S5–S6, conducts ions. BK has a large C-terminal region that contains target sequences for channel modulation such as a Ca^{2+} bowl, two domains that regulate the conductance of K^+ (RCK1 and RCK2), a tetramerization domain, leucine zipper motifs, a heme-binding motif, two phosphorylation sites, and a caveolin-targeting domain (2, see Ref. 3 for review). The leucine zipper motifs, contained in the C terminus, are essential for protein-protein interactions and modulating channel activity and expression.

Four genes, designated as *Kcnma*, encode the α-subunits of the different Slo channels. These include *Kcnma1* (Slo1), two similar paralogs, *Kcnma2* (Slo2.1 and Slo2.2), and *Kcnma3* (Slo3). The α-subunits form homotetramers that are K^+-selective, but differ in their gating properties (2). All α-sub-

[1] The abbreviations used are: BK, large conductance Ca^{2+}-activated K^+ channel; BKAP, BK-associated protein; Anxa5, annexin V; ApoA1, apolipoprotein A1; BiP, binding immunoglobulin protein; CaM, calmodulin; CHO, Chinese hamster ovary cells; CICR, Ca^{2+}-induced-Ca^{2+}-release; CRT, calreticulin; O/N, overnight; GAPDH, glyceraldehyde-3-phosphate dehydrogenase; GRP78, glucose-regulated protein 78; GST, glutathione *S*-transferase; HPCAL, hippocalcin; HSP, heat shock protein; IHC, inner hair cell; Lin 7c, lin7 homolog c; MP0, myelin P zero; OHC, outer hair cell; siRNA, silencing RNA; SOD, superoxide dismutase; VDAC, voltage-dependent anion channel; RT, reverse transcriptase; IEF, isoelectric focusing; HA, hemagglutinin; RNAi, RNA interference; ER, endoplasmic reticulum; ScrRNA, scrambled RNAs; RyR, ryanodine receptors; ROS, reactive oxygen species; NIHL, noise-induced hearing loss; LC-MS/MS, liquid chromatography tandem mass spectrometry; NMDA(R), *N*-methyl-D-aspartic acid (receptor); TRP, transient receptor potential; coIP, coimmunoprecipitation.

From the ‡Department of Otolaryngology – Head and Neck Surgery, University of South Florida, College of Medicine, Tampa, Florida 33612 and §European Bioinformatics Institute, Wellcome Trust Genome Campus, Hinxton Cambridge, CB10 1SD, United Kingdom

Received, October 30, 2008, and in revised form, May 6, 2009

Published, MCP Papers in Press, May 7, 2009, DOI 10.1074/mcp.M800495-MCP200

units have S1–S6 transmembrane domains, whereas only Slo1 and Slo3 have an additional S0 domain and a Ca^{2+} bowl that is composed of a majority of either positively (Slo1) or negatively charged (Slo3) amino acids.

BK channels are important to sensory or hair cell "tuning" in lower vertebrates. This function is reflected by the variations in channel kinetics found along the tonotopic gradient of the turtle cochlea, thereby contributing to differences in electrical resonance or tuning. In these vertebrates, BK is colocalized with L-type Ca^{2+} channels in presynaptic active zones (3) and is thus coupled to neurotransmitter release as described for the nerve muscle synapse (4, 5). Although the onset of this channel during cochlear development in both mammals and non-mammals coincides with an increase in hearing sensitivity (6, 7), its function is less clear in the former where hair cells are not frequency-tuned and studies report either the presence or the absence of hearing with the loss of BK (8, 9). The BK channel has been localized to both the outer hair cells (OHC) (10) and inner hair cells (IHC) (7, 11–13) in mammals. However, unlike non-mammals, the BK channel appears in both synaptic and extrasynaptic sites near the apical end or neck of the IHC (9).

More than 100,000 expressed sequence tags have been identified in the vertebrate cochlea (14), thus, the use of yeast two-hybrid screening to determine BKAPs is a difficult task. However, recent developments in proteomics in combination with immunoprecipitation and LC-MS/MS analysis, allow for the efficient identification of interacting partners. Thus far, more than forty different expressed sequence tags have been identified in other tissues; most of these proteins interact with the C terminus of the channel to modulate expression as well as function (15).

In the present study, we determined putative BKAPs in mouse cochlea by coIP and mass spectrometry followed by further validation using reciprocal coIP, colocalization, and siRNA. We identified 174 BKAPs in 30-day-old mouse cochlea, which were further analyzed using bioinformatics. A BK interactome revealed several insights into BK function and common cellular pathways and processes. This approach identified novel BKα complexes with important roles in development, calcium binding, and chaperone activity as well as hearing loss.

EXPERIMENTAL PROCEDURES

Coimmunoprecipitation—A total of 16 cochleae were excised from 30-day-old CBA/J mice and immersed in 100 μl of lysis buffer containing 50 mM Tris-HCl, pH 8.0, 120 mM NaCl, 5 mM EDTA, 50 mM NaF, 500 μg/ml AEBSF, 10 μg/ml leupeptin, 10 μg/ml pepstatin A, 2 μg/ml aprotinin, and 5 μM okadaic acid, as described previously (16) and sonicated (Sonic Dismembrator Model 100; Thermo Fisher). The resulting lysate was centrifuged for 2 min at 700 $\times$ *g* and the supernatant removed to another tube. The pellet was resuspended with 100 μl of lysis buffer, sonicated, and centrifuged again. The supernatant was removed and combined with the previous extract and centrifuged at 100 k $\times$ *g* for 1 h at 4 °C. The supernatant, comprising the cytoplasmic fraction, was transferred into a fresh tube and placed on ice.

Initial solubility tests of the membrane/cytoskeleton fraction, using detergents such as CHAPS, octyl β-glucoside, dodecyl β-maltopyranoside, and ASB-14 revealed that ASB-14 gave the best separation. Thus, this fraction was prepared by solubilizing the pellet in 130 μl of lysis buffer containing 0.1% ASB-14 (Calbiochem), followed by vortexing at 1500 rpm (MixMate, Eppendorf) for 10 min and agitating on a rocking shaker for 1 h at 4 °C. Both fractions were precleared using 10 μl of rec-Protein G-Sepharose 4B beads (Invitrogen) for 15 min. The cytoplasmic and membrane/cytoskeletal fractions were divided equally into four pairs of tubes, each set containing both fractions. One set served as the coIP proteins, the second as the total proteome, the third as a matrix bead control, and the fourth as an additional negative control, by using an antibody to the vesicular stomatitis virus (Bethyl Laboratories), which is nonspecific to the cochlea. Six μg of an anti-BKα polyclonal antibody (Chemicon; amino acid residues 1098–1196 of mouse Kcnma1) was added to fractions to be used for coIP. Samples were incubated with rocking for 1 h at 4 °C. Immunocomplexes from the coIP fractions were captured by adding 25 μl of protein G beads and rocking for 1 h at 4 °C. Another 25 μl of protein G beads were added to the matrix control fractions. Beads were washed with Tris-buffered saline/Tween 20 [50 mM Tris-HCl, pH 8.0, 150 mM NaCl, 0.1% Triton X-100] buffer four times to remove nonspecific proteins. Immunocomplexes were eluted by adding 62.5 μl of two-dimensional sample buffer [7 M urea, 2 M thiourea, 0.5% pI, 3/10 carrier ampholytes (Bio-Rad), 0.4% ASB-14 and protease/phosphatase inhibitors] and 62.5 μl of two-dimensional rehydration buffer [7 M urea, 2 M thiourea, 0.2% carrier ampholytes, 100 mM dithiothreitol, and 0.4% ASB-14]. Samples were vortexed and centrifuged at 1500 $\times$ *g* for 10 min at RT. The supernatant was aliquoted into separate tubes for proteomic analysis. Experiments were repeated four times, and results from at least two were sent for MS analysis.

PAGE and MS Analysis—IEF was performed using 7-cm immobilized pH gradient (IPG) gel strips, pH 3–10 (Protean IEF Cell System, Bio-Rad). Proteins were resolved by IEF in the first dimension and SDS-PAGE (12% acrylamide) in the second dimension. Precision Plus (Bio-Rad) molecular weight marker was used to determine relative mobilities. Gels were stained with Coomassie Brilliant Blue-R250, and images were captured using the Molecular Imager versa doc MP Imaging System (Bio-Rad). The resolution of the scanning gel was 53 μm, and images were processed with the standard version of PDQUEST software (Bio-Rad), which was used to identify spots by pI and molecular weight with the help of standards. Spot sets, common to both immunoprecipitated and matrix control gels were eliminated from further analysis. Gel images of non-immunoprecipitated (total proteome) and immunoprecipitated proteins were compared and spots common to both coimmunoprecipitated fractions were excised and subjected to reduction, alkylation, and trypsin digestion as described previously (16–17). Peptides were extracted and concentrated under vacuum centrifugation.

A nanoflow liquid chromatograph (1100, Agilent, Santa Clara, CA) coupled to an electrospray ion trap mass spectrometer fitted with a chip-based ion source (HCT Ultra, Agilent) was used for tandem mass spectrometry peptide sequencing experiments. Following capture on a C18 reverse phase trap column, peptides were separated with a C18 reverse phase analytical column using a 30 min gradient from 5% buffer A to 50% buffer B [buffer A: 2% acetonitrile/0.1% formic acid; buffer B: 90% acetonitrile/0.1% formic acid]. Trap and analytical columns were contained on an Agilent Protein Identification Chip (G4240–62002) that has a 40 ηl enrichment column and a 75 μm $\times$ 150 mm analytical column. Both columns were packed with 5-μm SB-Zorbax C-18 reverse phase medium. Loading was performed at 4 μl/min followed by valve switching and LC-MS/MS at 300 ηl/min. Five tandem mass spectra were acquired for each MS scan; prior precursors were excluded for 60 s.

The peaklist-generating software was DataAnalysis version 3.4 (Bruker Daltonic GmBH). Sequences were assigned using MASCOT version 2.1.03 search engine (Matrix Science) against the National Center for Biotechnology Information nonredundant database (NCBI nr 2006.12.05) selected for *Mus musculus* (107924 entries). Precursor mass tolerance was ± 2.5 Da (monoisotopic) and fragment ion tolerance was ± 0.80 Da (monoisotopic). No fixed modifications were selected. Variable modifications consisted of carbamidomethylation (C), carboxymethylation (C), and oxidation (M). A maximum of two missed tryptic cleavages were allowed. Peptide assignments were manually verified by inspection of the tandem mass spectra and consistency with expected gas phase fragmentation patterns. Scaffold (version 01 07 00; Proteome Software) was used to validate MS/MS peptides and for protein identification. A 95% confidence level was assigned for the score values of individual spectra, and peptides were selected as specified by the Peptide Prophet algorithm. In addition, a false discovery rate (*i.e.* false positives and negatives) was determined for the obtained spectra by sampling every fifth file against a database of reversed mouse sequences, using Scaffold for the analysis.

Database Analyses—The search for additional proteins (*i.e.* secondary) that interact with primary BKAPs was performed using the Envision tool to search the molecular interaction database IntAct (18). The search was limited to murine proteins and was not extended to orthologues in other species. Colocalization data (*e.g.* cosedimentation) were not included in the final results. Interaction networks were visualized, modeled, and analyzed using the program Cytoscape (19). Proteins in the network were labeled according to UniProtKB nomenclature and color-coded according to the fraction from which they were obtained (membrane/cytoskeleton *versus* cytoplasmic) as well as the database (*i.e.* IntAct) and subcellular localization.

Reciprocal Coimmunoprecipitation—Reciprocal coIPs were accomplished as described above, except that antibodies to various proteins determined as potential BKAPs from the MS analyses were used to immunoprecipitate BKα from combined membrane/cytoskeletal and cytoplasmic fractions prepared from cochlear tissues. Antibodies included anti-14-3-3 γ (BIOMOL); annexin V, apoA1, cofilin, lin 7c, γ-actin, GAPDH, GST, hippocalcin, MP0 (Abcam), and calmodulin (Invitrogen) antibodies. Immunoprecipitation was accomplished by using the immunocomplex capture technique. Five μg of antibody was added to the sample and incubated at 4 °C for 1 h with rocking. Beads were added and the sample again incubated for 1 h. Immunocomplexed beads were washed five times in lysis buffer, eluted in sample buffer (Sigma), and heated at 70 °C for 10 min. Samples were fractionated on a 10% SDS-PAGE gel and transferred to a nitrocellulose membrane (Protran BA; Schleicher & Schuell). Blots were blocked in phosphate-buffered saline/Tween 20 [100 mM phosphate buffer, pH 7.4, 150 mM NaCl, 0.1% Tween 20], containing 5% milk for 1 h, and probed with BKα polyclonal antibody at 1:250 (Chemicon), followed by donkey anti-rabbit horseradish peroxidase-conjugated secondary antibody at 1:6000 (Amersham Biosciences). Controls consisted of pre-adsorbing the anti-BKα antibody with antigen (3:1) for 1 h at RT, incubating samples with uncomplexed beads, and immunoprecipitating BKα using anti-BK antibody. Immunoreactive bands were developed using enhanced chemiluminescence (Amersham Biosciences). Magic Mark XP (Invitrogen) was used as the protein standard to estimate relative mobilities.

Immunohistochemistry and Confocal Imaging—Mice cochleae were isolated, dissected, and fixed O/N at 4 °C by immersion in 4% paraformaldehyde in 100 mM phosphate buffer, pH 7.4. Cochleae were decalcified in Cal-EX decalcifying solution (Fisher) for 15 min, cryoprotected in 30% sucrose overnight, and infiltrated in a 1:1 mixture of Tissue-Tek embedding medium (Sakura Fine-Tek) and 30% sucrose under vacuum for one hour. Cryosections of 20 μm thickness were collected. Sections were permeabilized with 0.3% Triton X-100, preblocked with 10% goat anti-mouse serum for 30 min, followed by blocking with 10% goat serum for 30 min. Antibodies used are mentioned previously, with the addition of an anti-VDAC antibody (Abcam) for the localization of mitochondria. The tissue sections were incubated O/N at 4 °C in primary antibody diluted in the blocking solution. Detection was performed using anti-mouse Alexa 594 (BK) and anti-rabbit Alexa 488 (BKAPs)-conjugated secondary antibodies (Invitrogen). Sections were mounted in Vectashield mounting medium containing 4′,6-diamidino-2-phenylindole (Vector Laboratories). No immunoreactivity was detected in the absence of the primary antibodies. Sections were imaged with a Leica SP5 AOBS tandem scanning inverted confocal microscope. Z-stacks were acquired using a step size of 0.2 μm.

Cloning and HA-tagging of a BKα Splice Variant from Mouse Cochlea—A mouse BK-DEC splice variant (GenBank accession no. FJ872117) was cloned from total RNA extracted from mouse cochlea by RT-PCR using a forward primer with a BglII restriction site, 5′-GGAAGATCTCCCAAGA TGGATGCGCTCATCA-3′ and a reverse primer, with a SalI restriction site, 5′ACGCGTCGACAGTTCTGG TCTCCTGGGAGT-3′. The PCR product was purified (QIAquick PCR purification kit; Qiagen) and cut at restriction sites BglII and SalI at 37 °C O/N. The insert was gel-purified (StrataPrep DNA gel extraction kit; Stratagene) and inserted into pcDNA3.1(+) (Invitrogen) at restriction sites BamHI (5′) and XhoI (3′). Tandem hemagglutinin (HA)-tagged BK vector was generated using the pcDNA3.1-BK-DEC variant as a PCR template. The forward primer, which included a HindIII (5′) site and a tandem HA-tagged sequence for linkage to the N terminus of BK-DEC, consisted of 5′-CCCAAGCTTACCATGGGATACCCTTACGACGTTCCTGATTACGCTTACC CTTACGACGTTCCTGATTACGCTATGGATGCGCTCATCATACCGGTGA-3′. The reverse primer was set for the BK HindIII site and consisted of 5′-CCCAAGCTTCACAAAACACAGCTC ACAAACAGTAGGGA-3′. The fragment was gel-purified and ligated into pcDNA3.1/BK-DEC. All primers were acquired from Integrated DNA Technologies.

Transfection of siRNA and BK-DEC—CHO cells were cultured in 60-mm dishes and maintained in minimal essential medium (α-MEM; Invitrogen) supplemented with 10% fetal bovine serum. Exogenous siRNAs to mouse CRT and GRP78/BiP (Stealth Select RNAi, Invitrogen) and HSP60 (Silencer Select RNAi, Ambion) were used in silencing studies along with ScrRNA (Stealth Select RNAi) that served as negative controls for low-, medium-, and high-GC content RNAi. Transfections were performed using 8 μl/plate of Lipofectamine2000 (Invitrogen), 1 μg of HA-tagged BK-DEC/pcDNA 3.1, and pooled siRNA concentrations of (μM): 150 CRT, 300 GRP78, and 500 HSP60, along with equal concentrations of scrambled RNAs. siRNAs were mixed in a 1:1:1 ratio targeted to the following sense strands (5′-3′) for CRT, UUAAAGAUGACAUGAACCUUCUUGG, AAAUCGGGCAUCUUGGCUUGUCUGC, and UUGUCUGGCCGCACAAUCAGUGUGU; GRP78, UGAUGUAUGCUCUUCACCAGUUGGG, UUUAUCUCCAAUCUGGUUCUUGAGA, and AGAACUUGAUGUCCUGCUGCACCGA; and HSP60 CCCUGAAUGAUGAGCUAGATT, GAAAGGGUGUCAUCACAGUTT, and UCAAAAGUGUGAAUUCCAATT. After 5 h of incubation, transfection medium was replaced with fresh supplemented α-MEM. After 48 h of incubation, the cells were harvested and sonicated on ice in lysis buffer. Lysates were centrifuged at 100 k $\times$ *g* for 20 min at 4 °C. Protein concentrations were determined by DC protein assay (Bio-Rad) per manufacturer's instructions. Forty μg of protein was fractionated on a 7.5% SDS-PAGE gel and transferred to a nitrocellulose membrane. Primary antibodies used were monoclonal anti-HA tagged (1: 5000; Sigma), polyclonal anti-CRT (1:1000; Abcam), polyclonal anti-GRP78 (1:500; Calbiochem), and polyclonal anti-HSP60 (1:30,000; Abcam). Immunoreactive bands were devel-

oped using enhanced chemiluminescence (Amersham Biosciences) and Magic Mark XP (Invitrogen) was used as the protein standard to estimate relative mobilities.

Mitochondrial Studies—Mitochondria were isolated from 16 mouse cochleae and from one mouse cerebellum using a kit per manufacturer's instructions (Qproteome, Qiagen). Briefly, cochlea and cerebellum were rapidly excised and stored at −80 °C. Tissues were rinsed in ice-cold phosphate-buffered saline, sonicated in lysis buffer containing a protease inhibitor mixture for 10 s on ice, and incubated end-over-end for 10 min. After a 10 min spin at 1000 × *g*, the pellet was resuspended in disruption buffer and triturated. The preparation was spun at 1000 × *g* for 10 min and the previous disruption step repeated. Supernatants were combined and centrifuged at 6000 × *g* for 10 min. The pellet was resuspended in purification buffer, layered on the surface of a density gradient, and spun at 20,800 × *g* for 15 min. Mitochondria were removed from the respective gradient, diluted in storage buffer, and spun at 8000 × *g* for 10 min. The pellet was resuspended in storage buffer and stored at −80 °C. Purified mitochondria were solubilized in lysis buffer and then incubated with 8 μg of polyclonal anti-BK antibody bound to protein G beads. Bound beads were washed five times in phosphate-buffered saline and eluted in boiling sample buffer followed by fractionating the eluate by SDS-PAGE on a 7.5% gel. Proteins were blotted and probed with anti-BK antibody (1:200) or with pre-adsorbed antibody (3:1).

CHO cells were transiently transfected with 1 μg of pcDNA3.1/BK-DEC in fusion, at the C terminus, with the fluorescent indicator mCerulean-C1 using Lipofectamine. After ~48 h, live cells were stained with MitoTracker Red CMX-ROS (Invitrogen) per manufacturer's instructions and viewed with a Leica SP5 confocal microscope. Cerulean was pseudo-colored dark green to visualize overlap with red.

RESULTS

Identification of BKAPs in Mouse Cochlea—BKAPs were identified in the mouse cochlea by using a combination of coIP, two-dimensional gel electrophoresis, and LC-MS/MS analysis. The overall schematic representation of the proteomics approach used is shown in Fig. 1*A*. An anti-BK α-subunit antibody was used to immunoprecipitate BK complexes from both membrane/cytoskeletal and cytoplasmic fractions. Protein profiles of mouse cochlea were obtained by isoelectric focusing followed by SDS-PAGE (Fig. 1, *B–E*). A total of 112 distinct spots from the membrane/cytoskeletal fraction and 71 from the cytoplasmic fraction were identified from the coIP assay using two independent LC-MS/MS analyses (Fig. 1, *B* and *C* and supplemental Tables 1 and 2), as compared with a total of 322 and 282 features found, respectively, for the non-immunoprecipitated fractions (Fig. 1, *D* and *E*). The majority of spots occurred in a wide range of molecular weights and isoelectric points (10–150 kDa and 4.0–8.5 pI). Once identified by MS, the variance between the observed (gel) and theoretical (MS) weights was ± 5 kDa when confirming protein names. Once redundant proteins were accounted for in the coIP-derived results, there were a total of 103 and 71 distinct proteins from membrane/cytoskeletal and cytoplasmic fractions, respectively. Of these 174 proteins, 118 had >10 tandem peptides that matched, while 141 had a MASCOT score of 300 with >8% sequence coverage. However, eight proteins were common to both cell fractions and included annexin V, γ-actin I propeptide, 14-3-3 isoforms, and calbindin.

In comparison, no protein features were observed in two-dimensional gels for matrix controls nor when using an antibody nonspecific to the cochlea vesicular stomatitis virus-G (supplemental Fig. 1). The false discovery rate was ~1% as a search through a database of reversed mouse sequences detected only three potentially reliable peptides. The assigned sequences had both b and y ions present in the mass tandem spectra and there were ≤ three modifications on the peptide. Moreover, none of the proteins identified in the reverse database achieved the MASCOT cutoff score set as a positive identification.

Reciprocal Coimmunoprecipitation Verification and Colocalization—To initially validate some of the findings, we used reciprocal coIP, using readily available antibodies. These studies were conducted for the following proteins: γ-actin, annexin V, apoA1, calmodulin, cofilin, 14-3-3 γ, GAPDH, glutathione *S*-transferase-Mu (GST-μ), hippocalcin, Lin7c, and MP0. Some of these proteins are known to interact with BK in other systems, whereas others are new associations. All of the proteins examined were able to immunoprecipitate the BK α-subunit, as identified by the polypeptide species seen at 110 kDa, when compared with an immunoprecipitation of BK. No immunoreactive band was observed in the pre-adsorption controls (Fig. 2).

BK is known to be present in not only the sensory cells but also in cells of the spiral ganglion, spiral ligament, and stria vascularis (20–22). The following BKAPs were examined with regard to their colocalization with BK in various cell types of the mouse cochlea: γ-actin, 14-3-3 γ, annexin V, apoA1, cofilin, Lin7c, GAPDH, GST-μ, hippocalcin-like 1, MP0, and calmodulin. These proteins were colocalized with BK in hair cells, ganglion cells, and stria vascularis, with examples shown for hair and ganglion cells (Fig. 3).

Network of Primary and Secondary Interactions—To further clarify the association of the primary BKAPs with BK, several analyses were accomplished using a bioinformatics approach, including searching for and mapping extended interactions and mining databases for prior ion channel interactions, subcellular localizations, and cellular process attributes. Firstly, we identified 174 primary proteins that associated with the BK α-subunit of mouse cochlea by coIP. These primary BKAPs were used to search the IntAct database for secondary protein-protein interactions. This search resulted in a total of 199 secondary proteins involved in 234 protein-protein interactions when limiting the search to only those interactions that were classified as physical, excluding cosedimentation (*i.e.* colocalization) data, and counting both A-B and B-A interactions (supplemental Table 3). A total of 84 of the same proteins from both primary and binary extended lists were found to interact with one another.

Cytoscape was used to visualize the network composed of primary and secondary interactions. This analysis revealed a

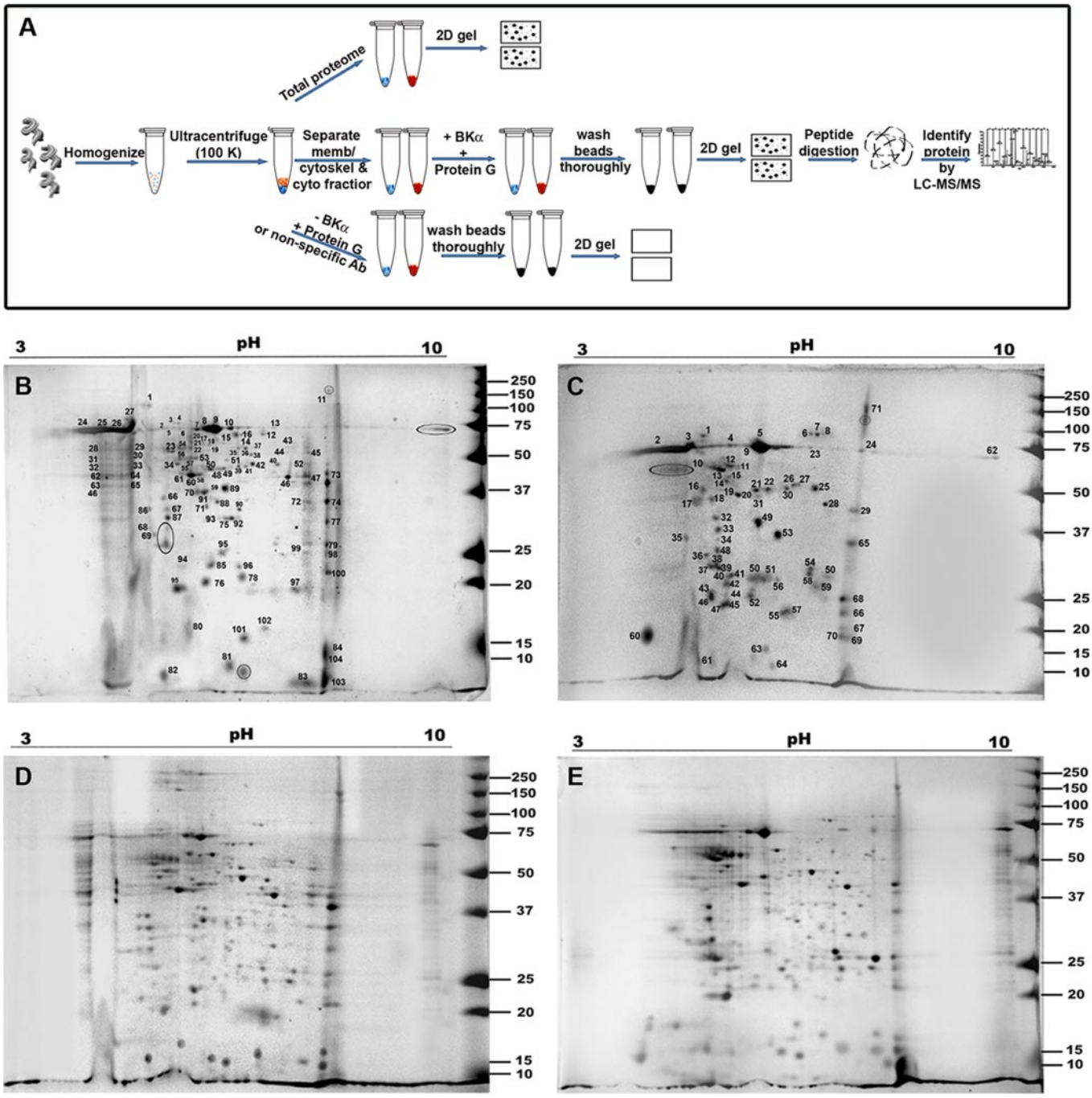

FIG. 1. **Schema and results of BKα coIP assay.** *A,* anti-BKα antibody bound to protein G beads was used to coimmunoprecipitate putative BKAPs from cochlear fractions. Resultant complexes were fractionated on a two-dimensional gel and analyzed using LC-MS/MS. Controls consisted of using membrane/cytoskeletal and cytoplasmic lysates in the absence of beads and antibody (total proteome), beads alone, or a nonspecific antibody (supplemental Fig. 1). Two-demensional gel electrophoresis of BKAPs for the membrane/cytoskeletal (*B*) and cytoplasmic fractions (*C*) shows 112 and 74 features resolved on these gels, respectively. All the numbered spots from the immunoprecipitated gels were subjected to LC-MS/MS analysis. Regions delimited by ovals represent proteins that are common to both fractions. Two-dimensional gel electrophoresis of the total proteome for the membrane/cytoskeletal (*D*) and cytoplasmic fractions (*E*) shows 322 and 282 visible features resolved on the gels, respectively.

network consisting of 199 nodes (proteins) and 234 edges (lines connecting nodes) (Fig. 4, *A* and *B*). Some nodes are connected by two edges in the network because this "double interaction" is a result of reciprocal verification in the IntAct database. We found that 87% of the proteins (160 nodes and 188 edges) are linked to form one large network (Fig. 4*A*). The

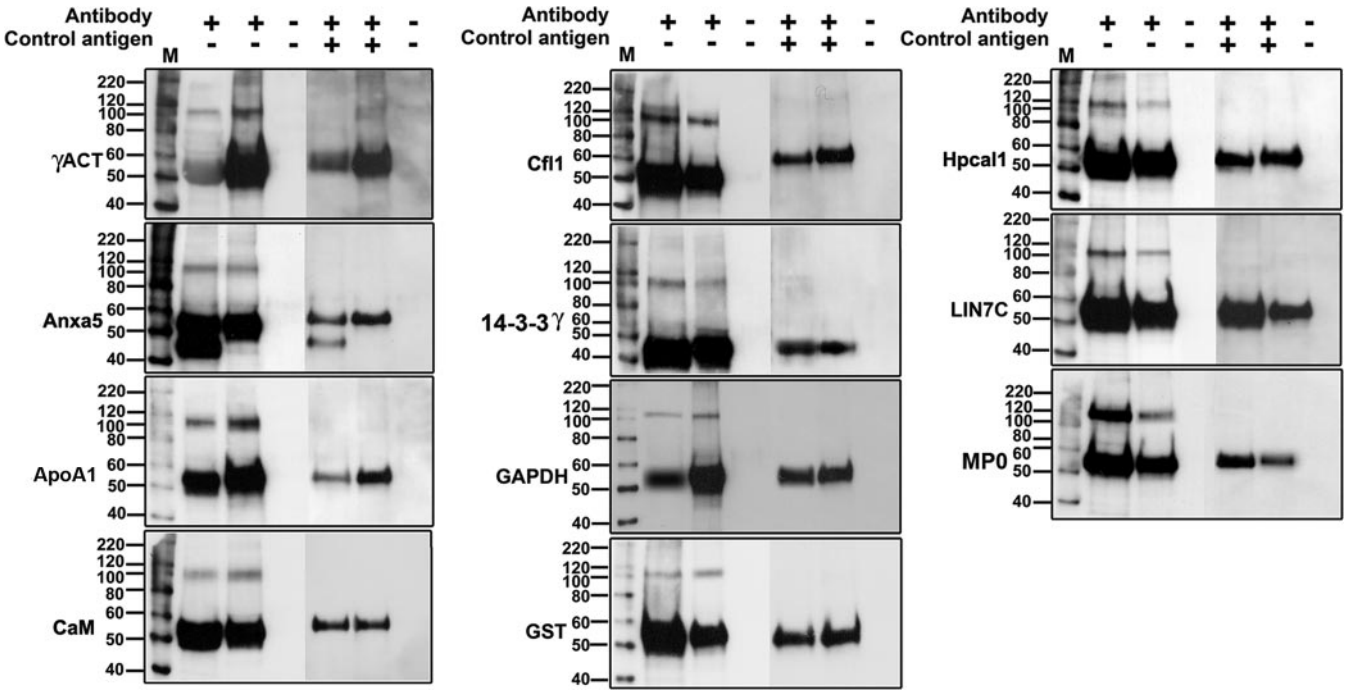

FIG. 2. **Verification of BKAPs by reciprocal coIP.** Eleven representative examples of BKAP reciprocal coIPs (*lane 2*; +,−) and BKα IPs (*lane 3*; +,−) reveal prominent immunoreactive peptide species of ~110 kDa, the expected weight of the BK α-subunit. The negative control, in which anti-BKα antibody was pre-adsorbed with peptide, did not produce immunoreactive bands for either the BKAP reciprocal coIPs (*lane 5*; +,+) or the BKα IPs (*lane 6*; +,+). The ~55 kDa bands correspond to heavy immunoglobulin (IgG), resulting from the use of polyclonal antibodies to both precipitate the proteins and probe the blots. Bead controls consisted of lysate mixed with protein G beads without antibody (*lanes 4* and *7*; −, −). The lane marked "*M*" is the molecular weight marker. BKAPs represented include γ-actin (*γACT*), annexin V (*Anxa5*), apolipoprotein A1 (*ApoA1*), calmodulin (*CaM*), cofilin (*Cfl1*), *14-3-3*γ, GAPDH, GST, hippocalcin 1 (*Hpcal1*), Lin7 homolog c (*LIN7C*), and myelin P0 (*MP0*).

remaining 13% are dispersed among 12 smaller networks composed of five nodes or less (Fig. 4*B*). Among the larger global network, of primary and secondary BKAPs, were twelve major hubs, containing a central protein connected to six or more partners, some of which were linked to the larger global network. There were 10 proteins central to these 12 hubs as some proteins, such as calmodulin, formed more than one hub. These central nodes included α-tubulin, ATP synthase β-subunit, calmodulin, calrecticulin, chromobox homolog 1, γ-actin, NMDA receptor, protein kinase ε, protein SET, and ubiquitin (Fig. 4*A*). All interacting proteins shown in the interactome are mouse proteins except for two, calmodulin and protein SET, which are shown as both human and mouse. This outcome was the result of affinity chromatography experiments using either mouse or human purified proteins, bound to the column, to capture mouse protein partners from lysates.

Prior Association of BKAPs with Ion Channels—The second approach was to manually search the literature to classify BKAPs by prior association with ion channels, subcellular localization, and cellular processes. This search revealed that ~63% of the BKAPs were reported previously to have an association with ion channels from different species and endorgans (Fig. 5*A*; supplemental Tables 4 and 5), whereas the remaining 37% were novel protein-ion channel (BK) interactions. These percentages were similar for the two cellular fractions examined. Of the known previous associations, K^+ and Ca^{2+} channels comprised the majority. In the membrane/cytoskeletal and cytoplasmic fractions, 16.5% and 19.7%, had prior associations with K^+ channels, whereas 25.2% and 16.9% had prior associations with Ca^{2+} channels, respectively. The remaining channel associations from each fraction were divided in descending order among BK (3.9%, 8.5%), TRP (4.9%, 4.2%), Cl^- (3.9%, 4.2%), VDAC (2.9%, 4.2%), Na^+ (3.9%, 1.4%), and other channels (*i.e.* aquaporin, nucleic acid, cationic; 0%–1.9%).

Subcellular Localization and Cellular Processes—Thirdly, BKAPs were examined with respect to their subcellular localization based on information from UniProtKB (Fig. 5*B*; supplemental Tables 4 and 5). Although various proteins may be found in different cellular compartments, the classification was based on the compartment in which the protein was primarily found. From the membrane/cytoskeletal fraction, a majority (38.8% and 21.4%) of the proteins were localized to the membrane and mitochondrion, respectively, whereas in the cytoplasmic fraction, 50.7% and 19.7% were localized to the cytoplasm and mitochondrion, respectively. Thus, in either fraction, a large portion of BKAPs were

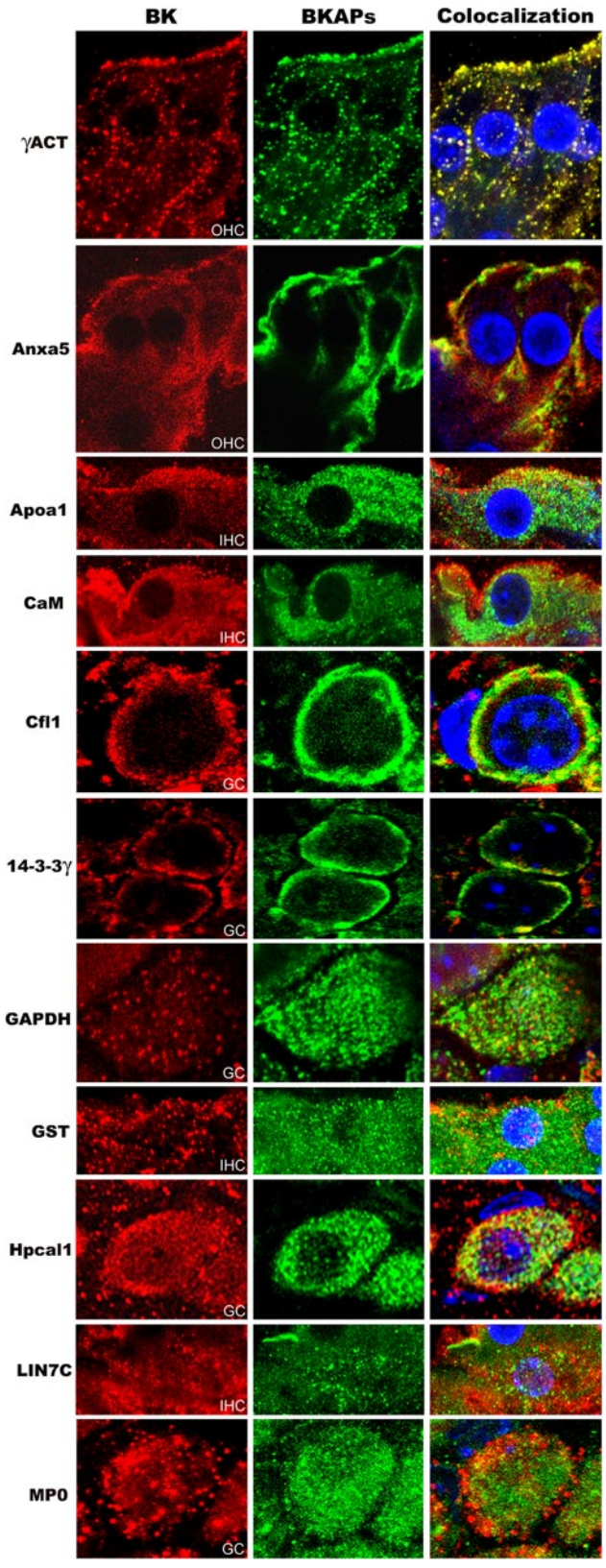

FIG. 3. **Coimmunolocalization of BKα and 11 BKAPs in various tissues from mouse cochlea.** Cochlear tissues were triple-stained for BKα (*red*), BKAPs (*green*), DAPI (*blue*), with colocalization shown in *orange* or *yellow*. Immunoreactivity for BKAPs and BKα is shown in IHC, OHC, and ganglion cells (*GC*). BKAPs colocalized with BK include γ-actin (γ*ACT*), annexin V (*Anxa5*), apolipoprotein A1 (*ApoA1*), CaM, cofilin (*Cfl1*), 14-3-3γ, GAPDH, GST, hippocalcin 1 (*Hpcal1*), Lin7 homolog c (*LIN7C*), and myelin P0 (*MP0*).

mitochondrial-related. Those falling in the next highest categories consisted of nucleus- (10.7%, 5.6%), secretory- (6.8%, 8.5%), ER- (8.7%, 4.2%), cytoskeletal- (6.8%, 4.2%), and Golgi- (4.9%, 5.6%)-related proteins. The fewest number of BKAPs were ribosomal- (1%, 0%) and peroxisomal-related (1%, 1.4%).

Fourthly, primary BKAPs were classified according to the cellular processes by manual data mining of the PubMed gene and literature databases and the Gene Ontology database (Fig. 5 *C*; supplemental Tables 4 and 5). BKAPs coimmunoprecipitated in the membrane/cytoskeletal and cytoplasmic fractions were associated with six specific cell processes. From both membrane/cytoskeletal and cytoplasmic fractions, a majority of proteins were involved in metabolism- (25.2%, 38%) and trafficking/scaffolding- (34%, 8.5%)-related processes. Among metabolically related proteins were SOD, a hearing loss-related protein, GST-μ, peroxiredoxin, and dehydrogenases such as dihydrolipoamide dehydrogenase and succinate dehydrogenase. Trafficking/scaffolding-related proteins included cofilin, tubulin, neurofilament, Lin7c, chaperone proteins of the HSP family, and γ-actin, a deafness-associated protein.

Developmental/differentiation processes (18.4%, 21.1%) were the third largest groups and contained proteins such as lamin A and C and valosin-containing protein, which were involved in neuronal growth, whereas myelin basic protein, myelin P0, and periaxin isoform L were known to play a vital role in the myelination of neurons. The final three groups included BKAPs that were associated with, in descending order, signaling (18.4%, 21.1%), transport (1.9%, 7%), and transcription/translation (1.9%, 4.2%). Signaling proteins included both proteins with Ca^{2+}-signaling/sensing functions as well as those involved in signal transduction, such as apolipoproteins and peroxiredoxin, respectively. BKAPs with a Ca^{2+}-binding function included hippocalcin-like 1, reticulocalbin 3 precursor, and calmodulin, among others. Transcription/translation and transport and proteins included synthesis initiation factor 4 A and calbindin2, respectively, with the latter acting as a Ca^{2+}-binding protein.

Silencing of Chaperonins—To determine whether BKα expression is altered by some of the discovered BKAPS, we chose the chaperonins as an example. These included calreticulin and GRP78, which are found along the protein-folding pathway in the endoplasmic reticulum (ER), and HSP60, which is closely linked to the mitochondria. For these experiments, we specifically examined the expression of an HA-tagged BK-DEC variant that was cloned from mouse cochlear tissues. The DEC refers to the sequence at

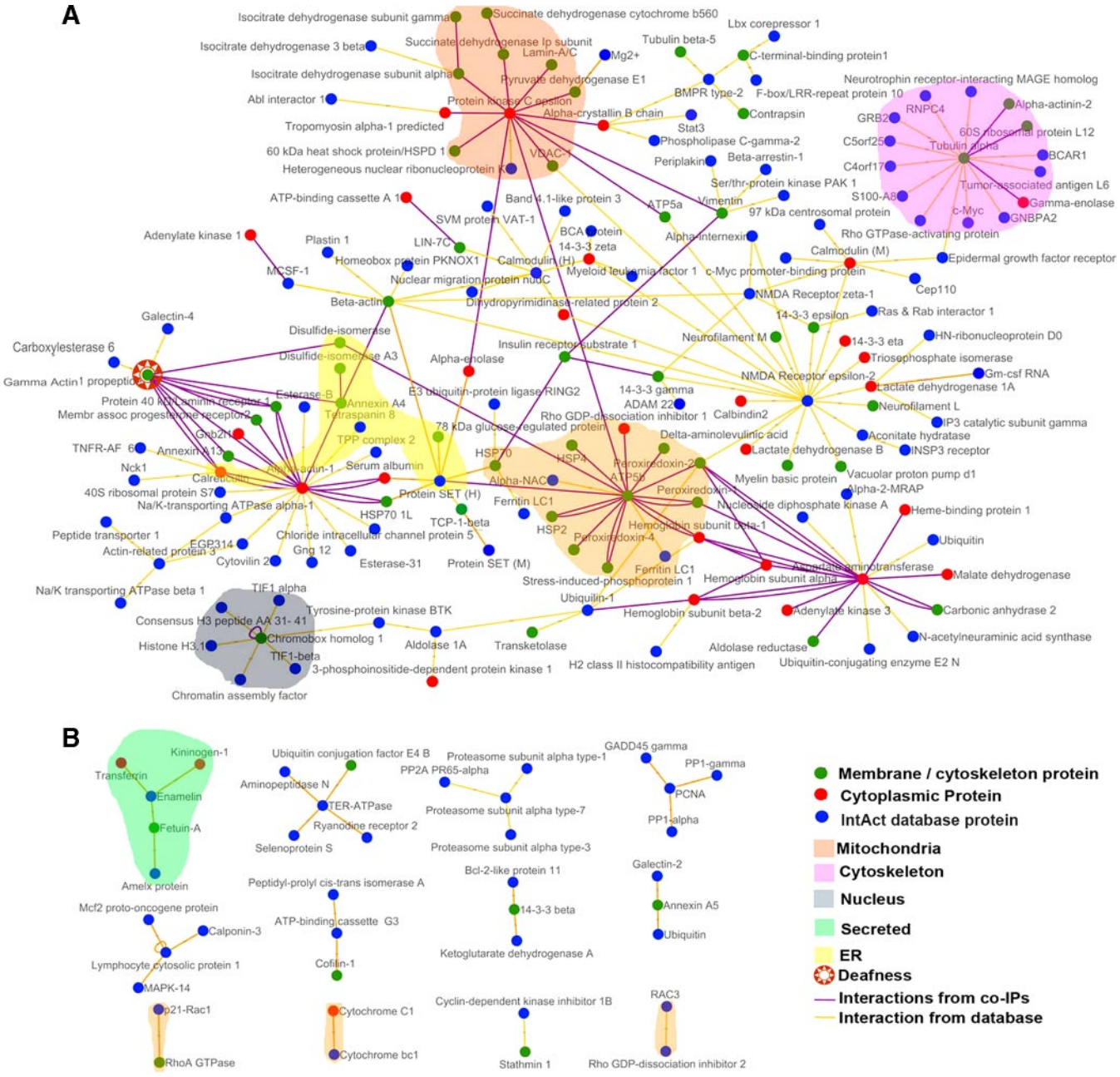

FIG. 4. **The BKAP interactome of mouse cochlea.** Visualization of primary and secondary BKAPs using Cytoscape revealed 13 networks involving 199 proteins and 254 interactions. *A,* of these proteins, 160 are nodes that are linked with 188 edges to form a single global network. Within this network are 12 major hubs consisting of a single node connected to six or more nodes that may or may not be linked to the larger network. The central nodes in these hubs include protein kinase C ε, α-tubulin, calmodulin, cytoplasmic actin, NMDA receptor, calreticulin, γ-actin, protein SET, ATP synthase β, ubiquitin, and chromobox homolog. *B,* the remaining BKAPs consist of 39 nodes and 28 edges that form 12 smaller distinct modules, each with five or fewer nodes. Different-colored nodes represent contributions from either membrane/cytoskeletal or cytoplasmic fractions or from the IntAct database source. Different-colored edges indicate interactions derived from the BKα coIP assays or from IntAct. Colored fields represent portions of the network that are located in different subcellular locations. BKAPs involved in deafness/NIHL are indicated by an additional symbol.

the very end of the C terminus. Under the culture conditions described above, treatment of endogenous calreticulin with siRNAs resulted in an ~50% knockdown of calreticulin, compared with CHO cells treated with ScrRNA (Fig. 6*A*). In turn, the reduction of calreticulin resulted in a >30% decrease in BK expression, 48 h after BK-DEC transfection and treatment with siRNA (Fig. 6*A*). A similar outcome was measured 48 h after CHO cells were treated with GRP78 siRNA and transfected with HA-tagged BK-DEC. Treatment of endogenous GRP78 with siRNAs resulted in an ~40%

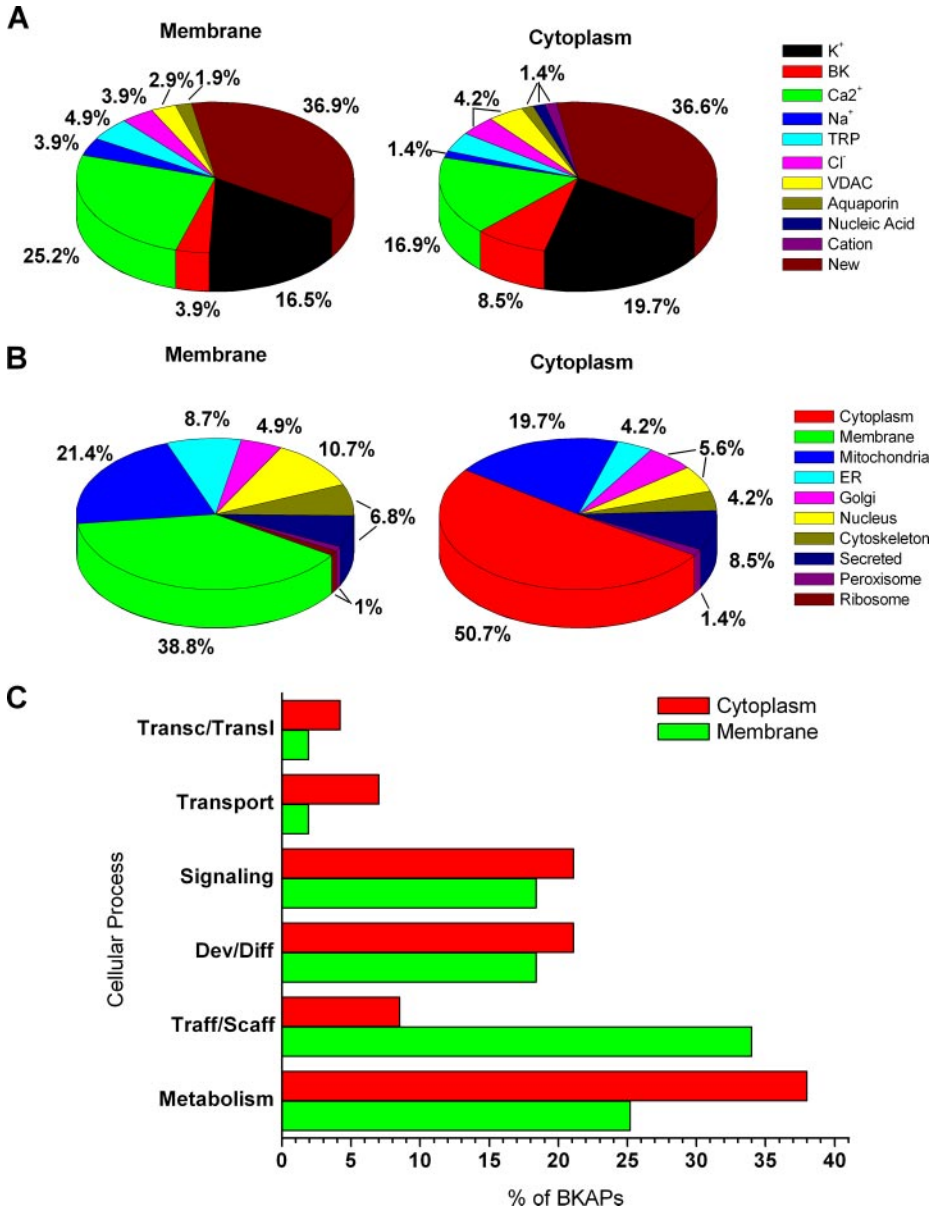

FIG. 5. **Primary BKAPs and their relation with ion channels, subcellular localization, and cellular process.** *A*, charts show previous ion channel associations of BKAPs as reported in PubMed for membrane/cytoskeleton and cytoplasmic fractions of mouse cochlea. The two major ion channel groups that show previous associations with BKAPs are K^+ and Ca^{2+} channels. However, ~37% of the putative isolated BKAPs have a new association with BK. The remaining BKAPs interact with TRP, Na^+, Cl^-, VDAC, aquaporin, nucleic acid, and cation channels. *B*, subcellular localization of BKAPs isolated from membrane/cytoskeletal and cytoplasmic fractions localized to various organelles and cellular matrices as determined by UniProtKB. Although a majority of BKAPs was found in the membrane and cytoplasm, a third major group was localized to the mitochondrion. Other proteins were dispersed among various organelles including ER, Golgi, and nucleus. *C*, BKAPs are classified according to the cellular process with which they are involved, as determined by mining Gene Ontology, GO Slim, and PubMed literature databases. A majority of BKAPS was involved in cellular processes related to metabolism and trafficking/scaffolding followed by development/differentiation, signaling, transport, and transcription/translation.

reduction in GRP78, compared with CHO cells treated with ScrRNA (Fig. 6*B*). This silencing in turn resulted in a >30% decrease in BK-DEC, 48 h after transfection (Fig. 6*B*). In contrast, silencing of endogenous HSP60 had an effect on BK-DEC that was opposite to the silencing of calreticulin and GRP78. An ~13% reduction in the expression of HSP60 resulted in a 26% increase in the overall expression of HA-tagged BK-DEC (Fig. 6*C*).

BK-DEC in Mitochondria—BKα was localized to the mitochondria both *in vivo* and *in vitro* (*i.e.* CHO cells) to further verify BKα in mitochondria. For this purpose, a BK-DEC variant was cloned from the cochlea and inserted in fusion with Cerulean. This variant was used to localize BK in CHO cells, using Mitotracker as a mitochondrial marker. Fig. 7 (*A* and *B*) shows the splice sequences for cloned BK-DEC and its localization (*yellow*) in the mitochondria of CHO cells, respectively. To verify BKα in the mitochondria of cochlear tissues, mitochondrial membrane was purified from whole cochlear lysate. The purified lysate was prepared for immunoblotting following immunoprecipitation, using an anti-BKα antibody, and compared with a similar preparation made from brain. The results show bands at the expected weight of ~110 kDa, for mitochondrial preparations made from cochlea and brain (Fig. 7*C*). In a final experiment, to colocalize BKα in hair cells, an anti-VDAC channel antibody was used as a marker for mitochondria because this channel was specific to this subcellular compartment. Using an anti-BKα antibody, BK was colocalized in the mitochondria with VDAC as seen by *yellow* fluorescence in an OHC (Fig. 7*D*).

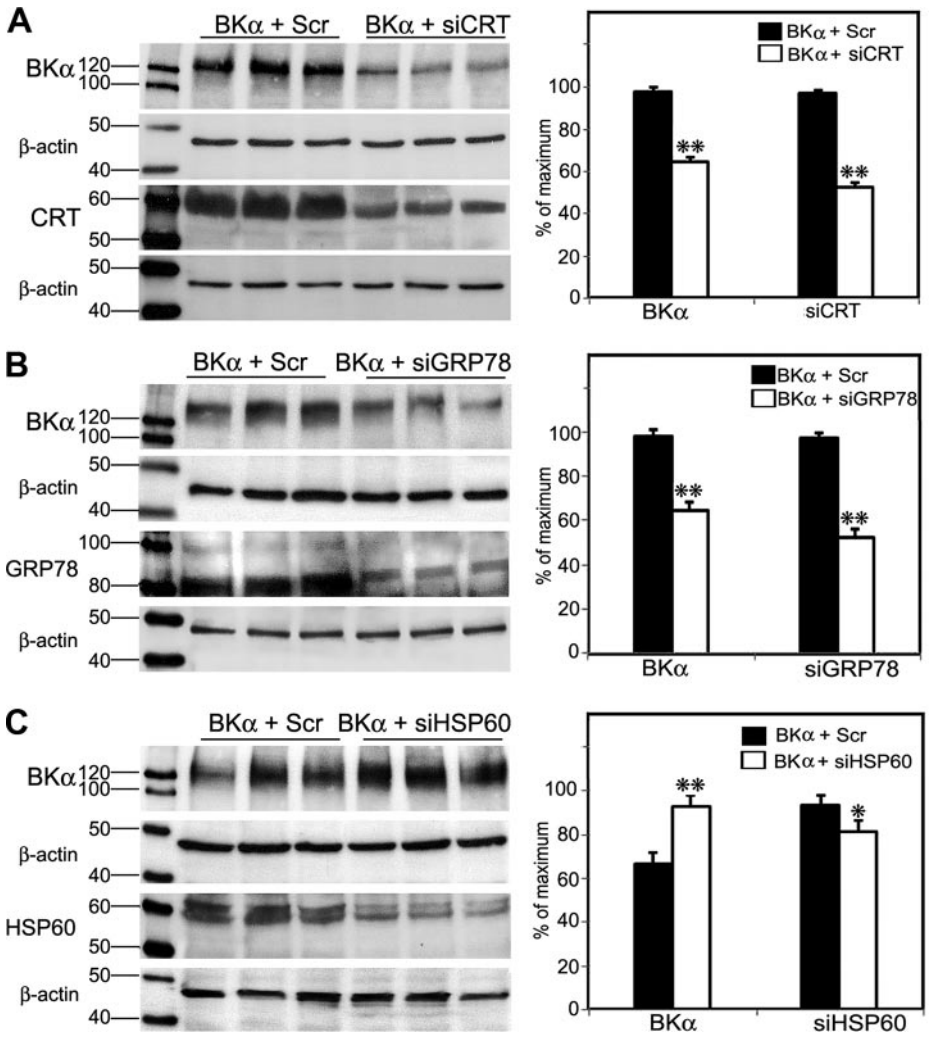

FIG. 6. **Regulation of BKα expression by chaperonins in CHO cells.** *A*, mouse siRNAs were used to reduce the expression of endogenous calreticulin (*CRT*) in cells transfected with BK-DEC (*BKα + SiCRT*). Controls consisted of CHO cells treated with BK-DEC and scrambled RNAs (*BKα + Scr*). Plots derived from densitometry measurements made for BKα and CRT show that a >30% reduction in BKα coincided with an ~50% reduction in CRT following 48 h of incubation. *B*, siRNAs reduced the expression of endogenous GRP78/BiP by ~40%, which resulted in a >30% decrease in BKα. Measurements for BKα and GRP78 were made relative to controls consisting of cells transfected with BK-DEC and ScrRNA. *C*, in contrast to the previous chaperonins, cells treated with HSP60 siRNA showed an ~13% reduction in HSP60 that resulted in a 26% increase in the expression of BKα. All lanes were loaded with equivalent amounts of protein that were calibrated as described under "Experimental Procedures." Experiments were done in triplicate as independent samples for both si- and ScrRNA groups and β-actin served as a loading control for all experiments. Densitometry measurements for each band in a lane were normalized to the highest densitometric value (normalized to 100%) within a given set of six lanes, consisting of triplicates for Scr- and siRNA-treated cells. Statistical significance was determined using an unpaired, two-tailed *t* test to obtain *, $p \leq 0.05$, **, $p \leq 0.001$. *Error bars* represent the standard error of the mean.

Summaries of some of the BKAPs from the interactome are illustrated with regard to their putative function and location in relation to the BK channel (Fig. 8). These locations include the plasmalemma, mitochondria, ER, and intracellular Ca^{2+} stores such as the subsurface cisternae.

DISCUSSION

Despite increased interest in the composition and function of BK in the vertebrate cochlea, there have been limited attempts to generate an in-depth proteome analysis. Previous studies reveal inner ear protein profiles using two-dimensional gels (20–24), whereas cisplatin-induced damage of proteins in the cochlea is identified by MALDI-TOF analysis (25). Using bioinformatic techniques, we demonstrated putative primary and binary protein-protein interactions of the BKα subunit in cochlea and harvested potentially relevant proteins involved in function, regulation, and metabolism.

Interestingly, in mammalian and non-mammalian vertebrates BK appears to be different in relation to its function in hair cells. In non-mammals, the BK channel underlies the electrical tuning of hair cells, allowing for the tonotopic organization of this sensory epithelium. In mammals, tonotopy is regulated primarily by the basilar membrane, as the hair cells are not electrically tuned. This difference is further underscored by the functional characterization of BK channels located both apically and basolaterally in the inner hair cells. Immunolocalization shows strong labeling in the neck and punctate labeling in the basolateral membrane (26). Patch clamp studies also reveal a functional difference in that BK channels are either activated by Ca^{2+} via influx through L-type Ca^{2+} channels or by intracellular stores (27). The latter Ca^{2+} source is likely related to those BK channels in the apex (28).

BK, Protein Folding, and Intracellular Ca^{2+} Stores—Approximately, 7% of putative BKAPs presented here can be localized to the ER or ER-like structures. Thus, the importance of these proteins may lie in the different functions attributed to these subcellular compartments. Among the proteins localized to the ER are the chaperonins, such as calreticulin and GRP78. These proteins are involved in folding linear amino acids into three-dimensional proteins. As BKα shuttles

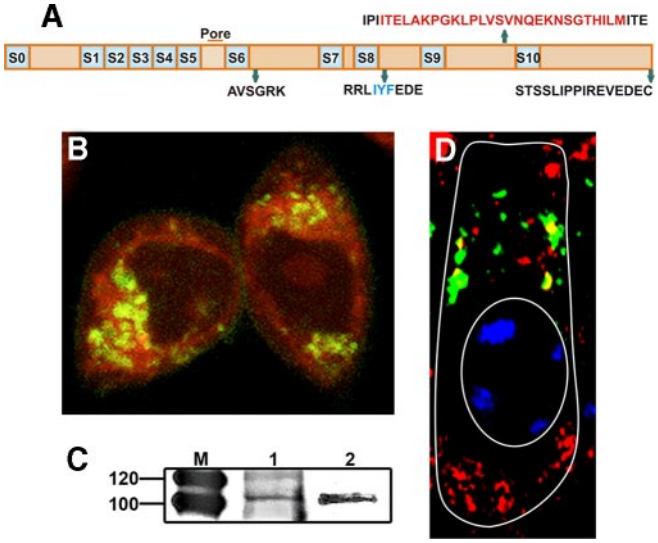

FIG. 7. **Expression of mitochondrial BKα *in vitro* and *in vivo*.** *A*, splice sequences shown in relation to the different regions of a BK-DEC variant cloned from mouse cochlea and used in CHO expression studies. *B*, live CHO cells transfected with pcDNA3.1 containing Cerulean in fusion with the C terminus of the BK-DEC variant and treated with MitoTracker (*red*) to identify mitochondria. Cerulean was pseudo-colored (*dark green*) to visualize overlap with *red* as *yellow*. *Dark green* immunostaining of BKα alone is observed at the plasmalemma. *C*, immunoprecipitation of BKα, using a pure mitochondrial preparation from mouse cochlea (*left lane*) and brain (*right lane*), shows bands at the expected weight of BK. *D*, tangential section of an outer hair cell, as outlined in *white*, showing the supranuclear region where BKα (*red*) is colocalized (*yellow*) in mitochondria with VDAC channels (*green*). The nucleus (*oval*) is partially stained with *blue* DAPI.

through the ER, both calreticulin and GRP78 have a direct effect on BK expression. As the results show, disruption of either protein via the RNA interference pathway causes a decrease in overall BKα expression.

The second type of ER likely involved with BKAPs is the cisternae, which are ER-like structures, found at the base and lateral sides of inner and outer hair cells (29), and contain ryanodine receptors (RyR). These structures regulate free cytosolic Ca^{2+}, and thus have a role in Ca^{2+}-induced-Ca^{2+}-release. Consequently, they may be necessary for the activation of BK channels localized in the supranuclear regions of the IHC membrane, as there appear to be two Ca^{2+} sources for the activation of BK channels in these cells. These include channels that use extracellular Ca^{2+} via L-type Ca^{2+} channels and others that appear to use intracellular stores of Ca^{2+} (27). Ryanodine is functionally coupled to BK channels in the smooth muscle of cerebral arteries (30), a scenario that may be similar in cochlea (31). However, the mechanisms for this coupling are unknown in either of these systems. Our results suggest several putative proteins, that may link BK with RyRs, including GST-μ, annexin, and CaM. GST is found in sensory cells of the Organ of Corti, localized to the apical region of both inner and outer hair cells (32). GST-μ regulates cardiac and skeletal RyR Ca^{2+} channels (33). In comparison, annexin not only functions in the release of Ca^{2+} from intracellular stores (34–35) but also acts as an organizer of membrane domains and trafficking of proteins (36). It may attach to the BK EF-hand domain, as annexins have a binding affinity for EF-hand Ca^{2+}-binding proteins. However, with channels such as TRP and TASK-1 the link occurs via an annexin subunit/complex known by the various names of S100A10/p11/annexin II light chain (37, 38). Of particular interest, in this dynamic, is that apolipoprotein binds to annexins in a Ca^{2+}-dependent manner (39). Recent data from this lab show that the apolipoprotein, apoA1, alters the biophysical characteristics of BK.[2] These results suggest that these three proteins, BK, apoA1, and annexin may form a triad that mediates Ca^{2+} release through RyR. Finally, CaM interacts with ryanodine receptors, acting as both an agonist and antagonist, depending on $[Ca^{2+}]_i$ and the type of RyR (40). CaM interacts with both SK and IK channels providing increased Ca^{2+} sensitivity (41). Although less is known of interactions between CaM and BK, Ca^{2+}/CaM kinase II activates BK to modulate neurotransmitter release, and there is evidence that CaM binding peptides bind BK (42, 43).

BK and Synaptic Sites—The connection of BK to Ca^{2+} channels at synaptic sites is documented for the cochlea as well as other systems. Among the BKAPs reported in the present study is the protein Lin7c/MALS3/VELIS3, a protein found at presynaptic sites. Its relation to Ca^{2+} channels in the cochlea likely lies in its interaction with β-catenin. The BKAP β-catenin was identified using BK as bait in a Y2H screening of a cochlea library (44). This study suggests that β-catenin may organize BK at these sites based on previous evidence. The PDZ heteromeric synaptic complex, of which β-catenin is a partner, is known to contain several Lin proteins including Lin7, which forms a complex with cadherin and needs β-catenin to move from the cytosol to these sites (45). Lin2, another partner of Lin7 in this complex, is known to bind to Ca_v channels (44, 46), thus potentially providing a link between Ca_v and BK. The function of the Lin7/BK interaction lies with previous evidence showing that the presence of Lin7 in the PDZ regulates the accumulation of binding partners at the presynaptic complex (45). This hypothesis is further underscored in that Lin7 indirectly mediates the polarized expression of K^+ channels in the basolateral membrane of renal epithelia, via association with Lin2 (47). Its function may be similar with the BK channel.

Maxi-K^+ channels possess a transmembrane voltage sensor, two distinct domains for K^+ conductance (RCK) and a Ca^{2+} bowl in the large intracellular C terminus. The Ca^{2+} bowl region is responsible for interacting with EF-hand Ca^{2+}-binding proteins. At least 12% of the proteins that coimmunoprecipitated with the anti-BK α-subunit were Ca^{2+}-binding pro-

[2] B. Sokolowski, K. Duncan, S. Chen, J. Karolat, T. Kathiresan, and M. Harvey, submitted for publication.

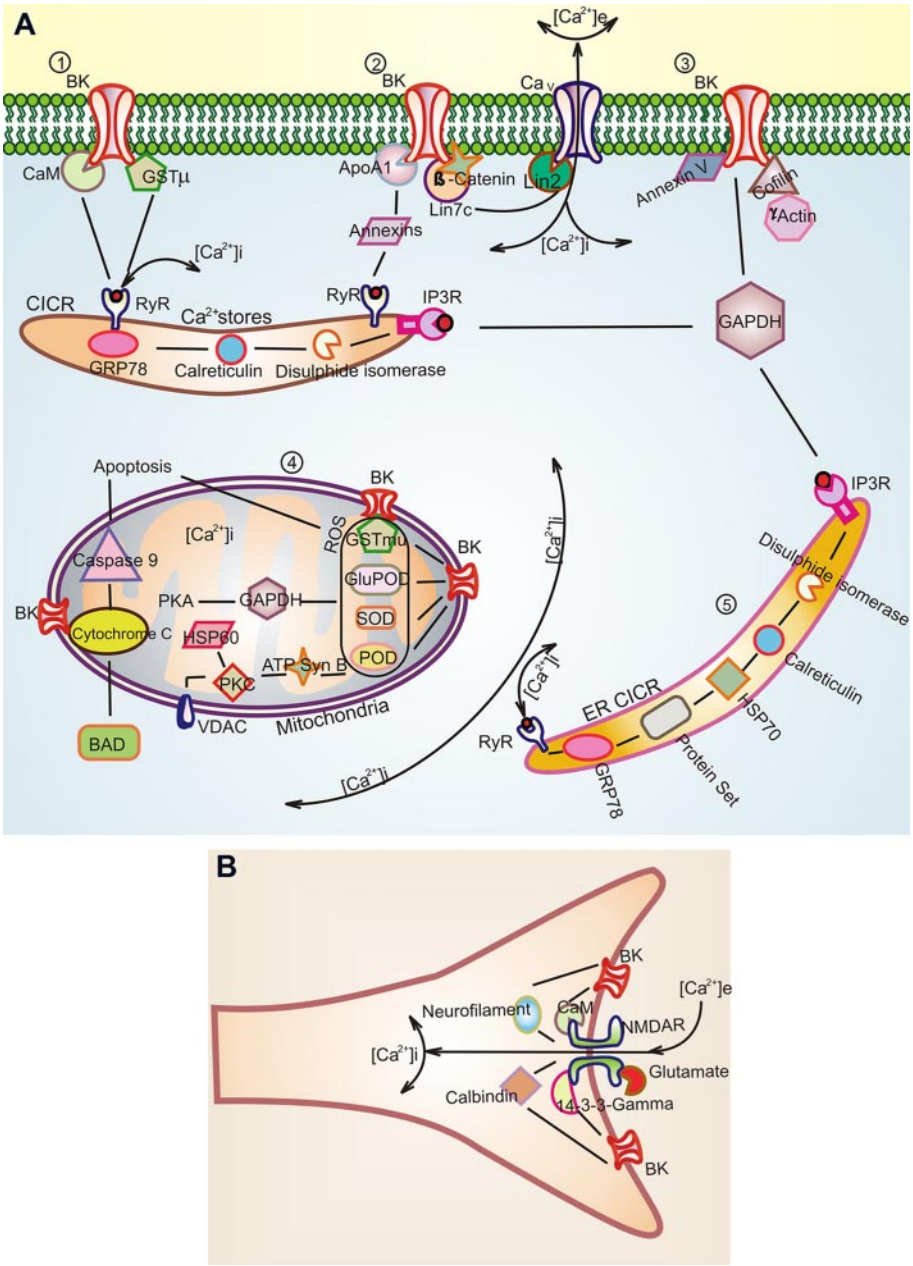

FIG. 8. **Putative BK-BKAP interactions derived from the BK interactome in mouse cochlea.** *A*, 1), putative primary BKAPs at the membrane include calmodulin, GSTμ, 14-3-3, ApoA1, γ-actin, Lin7c, annexin V, cofilin. BK channels are known to have a functional link to RyR (30) and, thus, possibly to intracellular stores. This link may occur via CaM or GSTμ. Another putative link is through annexin, which is known to regulate intracellular Ca^{2+} stores (34–35) and also binds to ApoA1 (39). ApoA1 alters the functional characteristics of BK. *A*, 2) Lin7, a primary BKAP, potentially interacts with BK as part of the Lin7·β-catenin complex. A BK link to Ca^{2+} channels in presynaptic sites may occur via the Lin7·Lin2 complex because Lin2 is known to interact with Ca^{2+} channels (46). *A*, 3) The cytoskeletal protein γ-actin and cofilin, a protein involved in disassembly of actin, are BKAPs that may link BK to the cytoskeleton. Thus, the link between BK and γ-actin may be disrupted in DFNA20/26, a mutation of γ-actin that causes deafness in humans. Protein 40 kDa and calreticulin are part of this matrix as determined from the interactome. *A*, 4) BKAPs associated with BK_{mito} may play a role in regulating intracellular Ca^{2+} in mitochondria, thus influencing apoptosis and phosphorylation. This premise is based on the interaction with cytochrome C, ATP synthase, and GAPDH, which regulate mitochondrial Ca^{2+}. BKα interactions with antioxidants such as SOD, GSTμ, and glutathione peroxidase (*GluPOD*) may be involved in mediating hair cell apoptosis initiated by the activation of ROS that can cause NIHL. The BKAP, cytochrome C, is shown in relation to BAD and Caspase-9, which are part of the hair cell apoptosis pathway (60). In addition, our data suggest HSP60 as a part of this pathway because it regulates BK expression inversely. *A*, 5) While the ER is another source for Ca^{2+}, here BKAPs such as GRP78 and calreticulin regulate the folding and assembly of BK. *B,* NMDAR is a binary partner of BK, forming a major hub in the BK interactome. There is a functional relationship to BK as NMDARs are known to provide an extracellular source for Ca^{2+} that activates BK. BKAPs common to both BKα and NMDAR include the structural and signaling proteins, neurofilament, and 14-3-3, respectively, and the Ca^{2+}-binding proteins, calbindin, and calmodulin.

teins. This group contains non-mitochondrial proteins that have EF-hand domains and include CaM, calbindin, and neuronal Ca^{2+} sensors, such as hippocalcin-like 1. Unlike CaM, members of the neuronal Ca^{2+} sensors act more as signaling switches rather than buffers because they bind Ca^{2+} above resting free Ca^{2+} levels and undergo conformational changes once bound (48). Previous evidence implicates BK interacting with myelin basic protein via CaM (15), whereas the other interactions are newly reported in the present study and require further experimentation with regard to their functions.

BK, Metabolism, and Mitochondria—Approximately 22% of the BKAPs in the present study have functions related to the mitochondrial membrane and matrix with ~ 7% related to the nucleus. BK channels have been reported in different cellular organelles, including the mitochondria of glioma, heart, brain, in addition to the nuclear envelope (49–52). The function and biological relevance of BK in these organelles is still uncertain because these discoveries are still in their early stages. Nonetheless, our data suggest that at least in cells of the cochlea there is a metabolic dynamic to BK that is in part mitochondrial-related. While, presently, there is no evidence of BK in the nuclear envelope of cochlear cells, there is initial evidence for BK in the mitochondria of hair cells, as identified by immunogold labeling[3] and by our experiments *in vitro* and *in vivo*. Furthermore, our data suggest that a possible candidate for BK_{mito} is the BKα splice variant known as BK-DEC. Previous studies show that BK-DEC has the least amount of expression at the plasmalemma relative to other variants such as BK-ERL and -VYR (53). Thus, its primary function may lie with subcellular components such as the mitochondria.

Among the putative BKAPs isolated are proteins found in the mitochondria, including HSP60, GAPDH, and the antioxidant enzymes peroxiredoxin, glutathione peroxidase, GST, and SOD. GAPDH and GST were verified by reciprocal coIP in our study, whereas the effect of SOD was demonstrated previously with tempol, a SOD mimetic that interacts with BKα in CHO cells, causing an increase in peak current (54). GAPDH is involved in oxidative phosphorylation (55), and its activation is one of the primary effects of Ca^{2+} influx into the mitochondrion (56–58). Thus, GAPDH gene expression in the Organ of Corti increases during ischemic conditions (59), a likely result of Ca^{2+} overload (60). Acoustic overstimulation induces the over-accumulation of Ca^{2+} in hair cell mitochondria, which in turn induces ROS (60) that can lead to hair cell apoptosis (61–62), as found in noise-induced hearing loss (NIHL). Antioxidants, such as glutathione (63) and superoxide dismutase (64), can control NIHL. BK interaction with these BKAPs may have a role in these effects as BK_{mito} is activated either under physiological or pathophysiological conditions that increase Ca^{2+} uptake and maintain homeostasis (65). Moreover, in brain and heart, BK_{mito} is protective in dealing with ischemia/ROS and/or apoptosis (65–68).

Interestingly, in cochlea, BK channels appear to have a role in acoustic overstimulation as demonstrated in BK knockouts, where the loss of this α-subunit results in a reduced sensitivity to NIHL (9). Although, the mechanism for this result is not understood, our HSP60 data provide possible links to this discovery. HSPs are associated with NIHL in humans (69), increase in response to acoustic overstimulation (70), and protect the cochlea from noise damage (71). In contrast to the outcome with calreticulin and GRP78, silencing of HSP60, in our study, resulted in an increase in BK expression. Thus, if HSP60 regulates BK in an inverse manner, an increase in HSPs with acoustic overstimulation should decrease BK expression, notably BK-DEC, and thereby protect the cochlea from noise damage.

BK, Structural Proteins, and Deafness—Among the cytoskeletal-related proteins identified as putative BKAPs were γ-actin and cofilin among others. Actins are among proteins important in the regulation of ion channels as well as hearing. BK is known to associate with both α- and γ-actin in the myometrium (2) and in conjunction with leptin it can cluster BK channels at synapses (72). Gamma-actin is a major cytoskeletal protein in cochlear sensory cells and missense mutations in its gene are associated with DFNA20/26, an autosomal dominant, nonsyndromic, sensorineural, hearing loss (73). Thus, it is likely this mutation would affect the expression of the BK channel as demonstrated by F-actin, which plays a role in the organization and reorganization of BK via an actin-binding domain at the C terminus of BK (74). Moreover, depolymerization of F-actin via cofilin leads to a reduction in Ca^{2+} currents regulated by L-type channels (75).

BK, Cell Signaling and Trafficking—Although not a primary BKAP, our results show NMDAR as a binary partner that forms the axis of one of the major hubs within the larger global network. Previous evidence suggests that Ca^{2+} influx through (NMDARs) is directly coupled to the activation of BK channels (76). The interactome revealed putative NMDA partners in common with the BK channel, including 14-3-3 ε, calbindin, and neurofilament L, among others. These BKAPs may link NMDARs to BK, for example, in dendritic endings of cochlear ganglion cells that contain this receptor (77, 78).

As described previously, BKα interacts with chaperones found in the ER and mitochondria. Chaperones made up ~3% of the BKAPs and also included HSP-70, HSP-90, and DNA-J proteins. HSPs play a role in K^+ channel tumor regulation (79), and both HSP70 and 90 are known to interact with ion channels such as HERG (80). Of these, HSP90 was isolated recently as a BK partner via the yeast two-hybrid system in our laboratory.[4] The DNA-J proteins likely act in conjunction with HSP in BK trafficking because the various homologs, dj1, dj2, and dj3, act as cochaperones for HSP proteins (81).

Our multiple proteomics approach provided insights into putative intracellular pathways regulating the BK α-subunit.

[3] R. Fettiplace, personal communication.

[4] B. Sokolowski, unpublished data.

While the bioinformatics approach revealed a number of potential secondary BK partners and their potential functions in the cochlea, there were certain inherent limitations. These limits included the use of different acronyms for individual proteins and a lack of annotations in protein databases because many interactions were not deposited in these datasets. Similar types of constraints are reported previously in a bioinformatics study of ion channel genes in the cochlea, where they affect a rigorous quantitative/statistical approach (14). Nonetheless, these data provide insights into BK function in mammalian hair cells that lie outside those of the plasmalemma, and may expand our ways of thinking about the importance of this channel in auditory sensory cells.

Acknowledgments—We thank Dr. John Koomen and Elizabeth Remily for help in data acquisition and analysis and Dr. Dave Piston for the gift of mCerulean-C1.

* This study was supported by National Institutes of Health/NIDCD Grant DC004295 (to B. S.). The Moffitt Proteomics Facility is supported by U. S. Army Medical Research Acquisition Activity Grant DAMD17-02-2-0051, NIH/NCI Grant P30-CA076292, and the Moffitt Foundation.

S The on-line version of this article (available at http://www.mcponline.org) contains supplemental material.

The interactions in this study have been submitted to the IMEx consortium through the IntAct database (Accession number IM-9475).

¶ To whom correspondence should be addressed: University of South Florida, Otology Laboratory, MDC83; 12901 Bruce B. Downs Blvd., Tampa, FL 33612. Tel.: 813-974-5988; Fax: 813-974-1483; E-mail: bsokolow@health.usf.edu.

REFERENCES

1. Marty, A. (1981) Ca-dependent K channels with large unitary conductance in chromaffin cell membranes. *Nature* **291,** 497–500
2. Brainard, A. M., Miller, A. J., Martens, J. R., and England, S. K. (2005) Maxi-K channels localize to caveolae in human myometrium: a role for an actin-channel-caveolin complex in the regulation of myometrial smooth muscle K+ current. *Am. J. Physiol. Cell Physiol.* **289,** C49–C57
3. Issa, N. P., and Hudspeth, A. J. (1994) Clustering of Ca^{2+} channels and $Ca(^{2+})$-activated K+ channels at fluorescently labeled presynaptic active zones of hair cells. *Proc. Natl. Acad. Sci.* **91,** 7578–7582
4. Robitaille, R., Adler, E. M., and Charlton, M. P. (1993) Calcium channels and calcium-gated potassium channels at the frog neuromuscular junction. *J. Physiol. Paris* **87,** 15–24
5. Pattillo, J. M., Yazejian, B., DiGregorio, D. A., Vergara, J. L., Grinnell, A. D., and Meriney, S. D. (2001) Contribution of presynaptic calcium-activated potassium currents to transmitter release regulation in cultured Xenopus nerve-muscle synapses. *Neuroscience* **102,** 229–240
6. Fuchs, P. A., and Sokolowski, B. H. (1990) The acquisition during development of Ca-activated potassium currents by cochlear hair cells of the chick. *Proc. Biol. Sci.* **241,** 122–126
7. Kros, C. J., Ruppersberg, J. P., and Rüsch, A. (1998) Expression of a potassium current in inner hair cells during development of hearing in mice. *Nature* **394,** 281–284
8. Rüttiger, L., Sausbier, M., Zimmermann, U., Winter, H., Braig, C., Engel, J., Knirsch, M., Arntz, C., Langer, P., Hirt, B., Müller, M., Köpschall, I., Pfister, M., Münkner, S., Rohbock, K., Pfaff, I., Rüsch, A., Ruth, P., and Knipper, M. (2004) Deletion of the Ca^{2+}-activated potassium (BK) alpha-subunit but not the BKbeta1-subunit leads to progressive hearing loss. *Proc. Natl. Acad. Sci.* **101,** 12922–12927
9. Pyott, S. J., Meredith, A. L., Fodor, A. A., Vázquez, A. E., Yamoah, E. N., and Aldrich, R. W. (2007) Cochlear function in mice lacking the BK channel alpha, beta1, or beta4 subunits. *J. Biol. Chem.* **282,** 3312–3324
10. Housley, G.D., and Ashmore, J.F. (1992) Ionic currents of outer hair cells isolated from the guinea-pig cochlea. *J. Physiol.* **448,** 73–98
11. Dulon, D., Sugasawa, M., Blanchet, C., and Erostegui, C. (1995) Direct measurements of Ca(2+)-activated K+ currents in inner hair cells of the guinea-pig cochlea using photolabile Ca2+ chelators. *Pflugers Arch.* **430,** 365–373
12. Oliver, D., Knipper, M., Derst, C., and Fakler, B. (2003) Resting potential and submembrane calcium concentration of inner hair cells in the isolated mouse cochlea are set by KCNQ-type potassium channels. *J. Neurosci.* **23,** 2141–2149
13. Skinner, L. J., Enée, V., Beurg, M., Jung, H. H., Ryan, A. F., Hafidi, A., Aran, J. M., and Dulon, D. (2003) Contribution of BK Ca^{2+}-activated K^+ channels to auditory neurotransmission in the guinea pig cochlea. *J. Neurophysiol.* **90,** 320–332
14. Gabashvili, I. S., Sokolowski, B. H., Morton, C. C., and Giersch, A. B. (2007) Ion channel gene expression in the inner ear. *J. Assoc. Res. Otolaryngol.* **8,** 305–328
15. Kim, H., Jo, S., Song, H. J., Park, Z. Y., and Park, C. S. (2007) Myelin basic protein as a binding partner and calmodulin adaptor for the BKCa channel. *Proteomics* **7,** 2591–2602
16. Kathiresan, T., Harvey, M. C., and Sokolowski, B. H. (2009) The use of two-dimensional gels to identify novel protein-protein interactions in the cochlea. In *Auditory/Vestibular Research, Methods and Protocols* (Sokolowski, B., ed.) pp. 269–286, Humana Press, New York
17. Krishnan, K., Kathiresan, T., Raman, R., Rajini, B., Dhople, V. M., Aggrawal, R. K., and Sharma, Y. (2007) Ubiquitous lens alpha-, beta-, and gamma-crystallins accumulate in anuran cornea as corneal crystallins. *J. Biol. Chem.* **282,** 18953–18959
18. Kerrien, S., Alam-Faruque, Y., Aranda, B., Bancarz, I., Bridge, A., Derow, C., Dimmer, E., Feuermann, M., Friedrichsen, A., Huntley, R., Kohler, C., Khadake, J., Leroy, C., Liban, A., Lieftink, C., Montecchi-Palazzi, L., Orchard, S., Risse, J., Robbe, K., Roechert, B., Thorneycroft, D., Zhang, Y., Apweiler, R., and Hermjakob, H. (2007) IntAct–open source resource for molecular interaction data. *Nucleic Acids Res.* **35,** D561–D565
19. Cline, M. S., Smoot, M., Cerami, E., Kuchinsky, A., Landys, N., Workman, C., Christmas, R., Avila-Campilo, I., Creech, M., Gross, B., Hanspers, K., Isserlin, R., Kelley, R., Killcoyne, S., Lotia, S., Maere, S., Morris, J., Ono, K., Pavlovic, V., Pico, A. R., Vailaya, A., Wang, P. L., Adler, A., Conklin, B. R., Hood, L., Kuiper, M., Sander, C., Schmulevich, I., Schwikowski, B., Warner, G. J., Ideker, T., and Bader, G. D. (2007) Integration of biological networks and gene expression data using Cytoscape. *Nat. Protoc.* **2,** 2366–2382
20. Adamson, C. L., Reid, M. A., Mo, Z. L., Bowne-English, J., and Davis, R. L. (2002) Firing features and potassium channel content of murine spiral ganglion neurons vary with cochlear location. *J. Comp. Neurol.* **447,** 331–350
21. Shen, Z., Liang, F., Hazen-Martin, D. J., and Schulte, B. A. (2004) BK channels mediate the voltage-dependent outward current in type I spiral ligament fibrocytes. *Hear. Res.* **187,** 35–43
22. Langer, P., Gründer, S., and Rüsch, A. (2003) Expression of Ca2-activated BK channel mRNA and its splice variants in the rat cochlea. *J. Comp. Neurol.* **455,** 198–209
23. Zheng, Q. Y., Rozanas, C. R., Thalmann, I., Chance, M. R., and Alagramam, K. N. (2006) Inner ear proteomics of mouse models for deafness, a discovery strategy. *Brain Res.* **1091,** 113–121
24. Thalmann, I. (2006) Inner ear proteomics: a fad or hear to stay. *Brain Res.* **1091,** 103–112
25. Coling, D. E., Ding, D., Young, R., Lis, M., Stofko, E., Blumenthal, K. M., and Salvi, R. J. (2007) Proteomic analysis of cisplatin-induced cochlear damage: methods and early changes in protein expression. *Hear. Res.* **226,** 140–156
26. Hafidi, A., Beurg, M., and Dulon, D. (2005) Localization and developmental expression of BK channels in mammalian cochlear hair cells. *Neuroscience* **130,** 475–484
27. Marcotti, W., Johnson, S. L., and Kros, C. J. (2004) Effects of intracellular stores and extracellular Ca(2+) on Ca(2+)-activated K(+) currents in mature mouse inner hair cells. *J. Physiol.* **557,** 613–633
28. Pyott, S. J., Glowatzki, E., Trimmer, J. S., and Aldrich, R. W. (2004) Extrasynaptic localization of inactivating calcium-activated potassium channels in mouse inner hair cells. *J. Neurosci.* **24,** 9469–9474
29. Grant, L., Slapnick, S., Kennedy, H., and Hackney, C. (2006) Ryanodine receptor localization in the mammalian cochlea: an ultrastructural study.

Hear. Res. **219,** 101–109
30. Pérez, G. J., Bonev, A. D., Patlak, J. B., and Nelson, M. T. (1999) Functional coupling of ryanodine receptors to KCa channels in smooth muscle cells from rat cerebral arteries. *J. Gen. Physiol.* **113,** 229–238
31. Beurg, M., Hafidi, A., Skinner, L. J., Ruel, J., Nouvian, R., Henaff, M., Puel, J. L., Aran, J. M., and Dulon, D. (2005) Ryanodine receptors and BK channels act as a presynaptic depressor of neurotransmission in cochlear inner hair cells. *Eur. J. Neurosci.* **22,** 1109–1119
32. el, Barbary, A., Altschuler, R. A., and Schacht, J. (1993) Glutathione S-transferases in the organ of Corti of the rat: enzymatic activity, subunit composition and immunohistochemical localization. *Hear. Res.* **71,** 80–90
33. Abdellatif, Y., Liu, D., Gallant, E. M., Gage, P. W., Board, P. G., and Dulhunty, A. F. (2007) The Mu class glutathione transferase is abundant in striated muscle and is an isoform-specific regulator of ryanodine receptor calcium channels. *Cell Calcium* **41,** 429–440
34. Díaz-Muñoz, M., Hamilton, S. L., Kaetzel, M. A., Hazarika, P., and Dedman, J. R. (1990) Modulation of Ca2+ release channel activity from sarcoplasmic reticulum by annexin VI (67-kDa calcimedin). *J. Biol. Chem.* **265,** 15894–15899
35. Arcuri, C., Giambanco, I., Bianchi, R., and Donato, R. (2002) Annexin V, annexin VI, *S100A1* and S100B in developing and adult avian skeletal muscles. *Neuroscience* **109,** 371–388
36. Gerke, V., Creutz, C. E., and Moss, S. E. (2005) Annexins: linking Ca2+ signalling to membrane dynamics. *Nat. Rev. Mol. Cell Biol.* **6,** 449–461
37. Girard, C., Tinel, N., Terrenoire, C., Romey, G., Lazdunski, M., and Borsotto, M. (2002) p11, an annexin II subunit, an auxiliary protein associated with the background K+ channel, TASK-1. *EMBO J.* **21,** 4439–4448
38. van de Graaf, S. F., Hoenderop, J. G., and Bindels, R. J. (2006) Regulation of TRPV5 and TRPV6 by associated proteins. *Am. J. Physiol. Renal Physiol.* **290,** F1295–F1302
39. Brownawell, A. M., and Creutz, C. E. (1996) Calcium-dependent binding of the plasma protein apolipoprotein A-I to two members of the annexin family. *Biochemistry* **35,** 6839–6845
40. Zalk, R., Lehnart, S. E., and Marks, A. R. (2007) Modulation of the ryanodine receptor and intracellular calcium. *Annu. Rev. Biochem.* **76,** 367–385
41. Lee, W. S., Ngo-Anh, T. J., Bruening-Wright, A., Maylie, J., and Adelman, J. P. (2003) Small conductance Ca2+-activated K+ channels and calmodulin: cell surface expression and gating. *J. Biol. Chem.* **278,** 25940–25946
42. Braun, A. P., Heist, E. K., and Schulman, H. (2000) Inhibition of a mammalian large conductance, calcium-sensitive K+ channel by calmodulin-binding peptides. *J. Physiol.* **527,** 479–492
43. Liu, Q., Chen, B., Ge, Q., and Wang, Z. W. (2007) Presynaptic Ca2+/calmodulin-dependent protein kinase II modulates neurotransmitter release by activating BK channels at Caenorhabditis elegans neuromuscular junction. *J. Neurosci.* **27,** 10404–10413
44. Lesage, F., Hibino, H., and Hudspeth, A. J. (2004) Association of beta-catenin with the alpha-subunit of neuronal large-conductance Ca2+-activated K+ channels. *Proc. Natl. Acad. Sci. U. S. A.* **101,** 671–675
45. Perego, C., Vanoni, C., Massari, S., Longhi, R., and Pietrini, G. (2000) Mammalian LIN-7 PDZ proteins associate with beta-catenin at the cell-cell junctions of epithelia and neurons. *EMBO J.* **19,** 3978–3989
46. Maximov, A., Südhof, T. C., and Bezprozvanny, I. (1999) Association of neuronal calcium channels with modular adaptor proteins. *J. Biol. Chem.* **274,** 24453–24456
47. Alewine, C., Kim, B. Y., Hegde, V., and Welling, P. A. (2007) Lin-7 targets the Kir 2.3 channel on the basolateral membrane via a L27 domain interaction with CASK. *Am. J. Physiol. Cell Physiol.* **293,** C1733–C1741
48. Burgoyne, R. D., and Weiss, J. L. (2001) The neuronal calcium sensor family of Ca2+-binding proteins. *Biochem. J.* **353,** 1–12
49. Siemen, D., Loupatatzis, C., Borecky, J., Gulbins, E., and Lang, F. (1999) Ca2+-activated K channel of the BK-type in the inner mitochondrial membrane of a human glioma cell line. *Biochem. Biophys. Res. Commun.* **257,** 549–554
50. Sato, T., Saito, T., Saegusa, N., and Nakaya, H. (2005) Mitochondrial Ca2+-activated K+ channels in cardiac myocytes: a mechanism of the cardioprotective effect and modulation by protein kinase A. *Circulation* **111,** 198–203
51. Douglas, R. M., Lai, J. C., Bian, S., Cummins, L., Moczydlowski, E., and Haddad, G. G. (2006) The calcium-sensitive large-conductance potassium channel (BK/MAXI K) is present in the inner mitochondrial membrane of rat brain. *Neuroscience* **139,** 1249–1261
52. Yamashita, M., Sugioka, M., and Ogawa, Y. (2006) Voltage- and Ca2+-activated potassium channels in Ca2+ store control Ca2+ release. *FEBS J.* **273,** 3585–3597
53. Kim, E. Y., Ridgway, L. D., Zou, S., Chiu, Y.-H., and Dryer, S. E. (2007) Alternatively spliced C-terminal domains regulate surface expression of large conductance calcium-activated potassium channels. *Neuroscience* **146**, 1652–1661
54. Xu, H., Bian, X., Watts, S. W., and Hlavacova, A. (2005) Activation of vascular BK channel by tempol in DOCA-salt hypertensive rats. *Hypertension* **46,** 1154–1162
55. Boulatnikov, I. G., Nadeau, O. W., Daniels, P. J., Sage, J. M., Jeyasingham, M. D., Villar, M. T., Artigues, A., and Carlson, G. M. (2008) The regulatory beta subunit of phosphorylase kinase interacts with glyceraldehyde-3-phosphate dehydrogenase. *Biochemistry* **47,** 7228–7236
56. Balaban, R. S. (2002) Cardiac energy metabolism homeostasis: role of cytosolic calcium. *J. Mol. Cell. Cardiol.* **34,** 1259–1271
57. Kovacs, G. G., Zsembery, A., Anderson, S. J., Komlosi, P., Gillespie, G. Y., Bell, P. D., Benos, D. J., and Fuller, C. M. (2005) Changes in intracellular Ca2+ and pH in response to thapsigargin in human glioblastoma cells and normal astrocytes. *Am. J. Physiol. Cell Physiol.* **289,** C361–C371
58. Sack, M. N. (2006) Mitochondrial depolarization and the role of uncoupling proteins in ischemia tolerance. *Cardiovasc. Res.* **72,** 210–219
59. Mazurek, B., Rheinländer, C., Fuchs, F. U., Amarjargal, N., Kuban, R. J., Ungethüm, U., Haupt, H., Kietzmann, T., and Gross, J. (2006) Influence of ischemia/hypoxia on the HIF-1 activity and expression of hypoxia-dependent genes in the cochlea of the newborn rat. *HNO* **54,** 689–697
60. Vicente-Torres, M. A., and Schacht, J. (2006) A BAD link to mitochondrial cell death in the cochlea of mice with noise-induced hearing loss. *J. Neurosci. Res.* **83,** 1564–1572
61. Lahne, M., and Gale, J. E. (2008) Damage-induced activation of ERK1/2 in cochlear supporting cells is a hair cell death-promoting signal that depends on extracellular ATP and calcium. *J. Neurosci.* **28,** 4918–4928
62. Kitahara, T., Li-Korotky, H. S., and Balaban, C. D. (2005) Regulation of mitochondrial uncoupling proteins in mouse inner ear ganglion cells in response to systemic kanamycin challenge. *Neuroscience* **135,** 639–653
63. Ohinata, Y., Yamasoba, T., Schacht, J., and Miller, J. M. (2000) Glutathione limits noise-induced hearing loss. *Hear. Res.* **146,** 28–34
64. Fortunato, G., Marciano, E., Zarrilli, F., Mazzaccara, C., Intrieri, M., Calcagno, G., Vitale, D. F., La, Manna, P., Saulino, C., Marcelli, V., and Sacchetti, L. (2004) Paraoxonase and superoxide dismutase gene polymorphisms and noise-induced hearing loss. *Clin. Chem.* **50,** 2012–2018
65. O'Rourke, B. (2007) Mitochondrial ion channels. *Annu. Rev. Physiol.* **69,** 19–49
66. Cheng, Y., Gu, X. G., Bednarczyk, P., Wiedemann, G. G., Haddad, G. G., and Siemen, D. (2008) Hypoxia increases activity of the BK channel in the inner mitochondrial membrane and reduces activity of the permeability transition pore. *Cell. Physiol. Biochem.* **22,** 127–136
67. Kulawiak, B., Kudin, A. P., Szewczyk, A., and Kunz, W. S. (2008) BK channel openers inhibit ROS production of isolated rat brain mitochondria. *Exp. Neurol.* **212,** 543–547
68. Sakamoto, K., Ohya, S., Muraki, K., and Imaizumi, Y. (2008) A novel opener of large-conductance Ca(2+)-activated K(+) (BK) channel reduces ischemic injury in rat cardiac myocytes by activating mitochondrial K(Ca) channel. *J. Pharmacol. Sci.* **108,** 135–139
69. Konings, A., Van, Laer, L., Michel, S., Pawelczyk, M., Carlsson, P. I., Bondeson, M. L., Rajkowska, E., Dudarewicz, A., Vandevelde, A., Fransen, E., Huyghe, J., Borg, E., Sliwinska-Kowalska, M., and Van, Camp, G. (2009) Variations in HSP70 genes associated with noise-induced hearing loss in two independent populations. *Eur. J. Hum. Genet.* **17,** 329–335
70. Lim, H. H., Jenkins, O. H., Myers, M.W., Miller, J. M., and Altschuler, R. A. (1993) Detection of HSP72 synthesis after acoustic overstimulation in rat cochlea. *Hear. Res.* **69,** 146–150
71. Yoshida, N., Kristiansen, A., and Liberman, M. C. (1999) Heat stress and protection from permanent acoustic injury. *J. Neurosci.* **19,** 10116–10124
72. O'Malley, D., Irving, A. J., and Harvey, J. (2005) Leptin-induced dynamic alterations in the actin cytoskeleton mediate the activation and synaptic clustering of BK channels. *FASEB J.* **19,** 1917–1919
73. Zhu, M., Yang, T., Wei, S., DeWan, A. T., Morell, R. J., Elfenbein, J. L.,

Fisher, R. A., Leal, S. M., Smith, R. J., and Friderici, K. H. (2003) Mutations in the gamma-actin gene (ACTG1) are associated with dominant progressive deafness (DFNA20/26). *Am. J. Hum. Genet.* **73,** 1082–1091
74. Zou, S., Jha, S., Kim, E. Y., and Dryer, S. E. (2008) A novel actin-binding domain on Slo1 calcium-activated potassium channels is necessary for their expression in the plasma membrane. *Mol. Pharmacol.* **73,** 359–368
75. Rueckschloss, U., and Isenberg, G. (2001) Cytochalasin D reduces Ca2+ currents via cofilin-activated depolymerization of F-actin in guinea-pig cardiomyocytes. *J. Physiol.* **537,** 363–370
76. Isaacson, J. S., and Murphy, G. J. (2001) Glutamate-mediated extrasynaptic inhibition: direct coupling of NMDA receptors to Ca(2+)-activated K+ channels. *Neuron* **31,** 1027–1034
77. Kuriyama, H., Albin, R. L., and Altschuler, R. A. (1993) Expression of NMDA-receptor mRNA in the rat cochlea. *Hear. Res.* **69,** 215–220
78. Niedzielski, A. S., and Wenthold, R. J. (1995) Expression of AMPA, kainate, and NMDA receptor subunits in cochlear and vestibular ganglia. *J. Neurosci.* **15,** 2338–2353
79. Han, X., Wang, F, Yao, W., Xing, H., Weng, D., Song, X., Chen, G., Xi, L., Zhu, T., Zhou, J., Xu, G., Wang, S., Meng, L., Iadecola, C., Wang, G., and Ma, D. (2007) Heat shock proteins and p53 play a critical role in K+ channel-mediated tumor cell proliferation and apoptosis. *Apoptosis* **12,** 1837–1846
80. Ficker, E., Dennis, A. T., Wang, L, and Brown, A. M. (2003) Role of the cytosolic chaperones Hsp70 and Hsp90 in maturation of the cardiac potassium channel HERG. *Circ. Res.* **92,** e87–e100
81. Terada, K., and Mori, M. (2000) Human DnaJ homologs dj2 and dj3, and bag-1 are positive cochaperones of hsc70. *J. Biol. Chem.* **275,** 24728–24734